Inhomogeneity as a source of collapse and revival for large-amplitude chirped coherent A_{1g} phonons in bismuth

O. V. Misochko, M. V. Lebedev, and E. V. Lebedeva
Institute of Solid State Physics, Russian Academy of Sciences, 142432 Chernogolovka, Moscow Region, Russia
(Received 21 April 2014; revised manuscript received 20 June 2014; published 2 July 2014)

We report a spatially resolved femtosecond pump-probe measurement of the lattice dynamics in bismuth made at helium temperature over a wide range of excitation levels. We demonstrate that the collapse and revival of chirped coherent A_{1g} phonons arises due to laterally inhomogeneous excitation conditions, whereas their enhanced decay can be due to potential damping.

DOI: 10.1103/PhysRevB.90.014301 PACS number(s): 78.47.J−, 63.20.Ry, 63.90.+t

I. INTRODUCTION

Ultrafast laser pulses, with durations shorter than typical nuclear vibrations, are widely used to prepare specific condensed matter states that would be otherwise inaccessible. Moreover, the same pulses can be used to study the evolution of the created state in real time. One of the effects of an ultrashort laser pulse incident on a crystal is the inducement of nonstationary lattice states (phonon coherence) in either the ground or excited electronic states [1]. Ground state coherence, usually ascribed to impulsive stimulated Raman scattering, is the dominant contribution in transparent materials, whereas lattice coherence in the excited electronic state is the main contribution for opaque crystals that have long-lived electronic excited states. Among the latter crystals, the most studied one in the time domain is Bi [1]. Bismuth has two atoms in the unit cell, and from simple electron counting it should be a semiconductor [2]. But due to the Peierls distortion along the trigonal axis coinciding with a fully symmetric A_{1g} phonon and the trigonal shift in a perpendicular direction corresponding to a doubly degenerate E_g phonon, the crystal becomes a semimetal [2,3]. At helium temperature bismuth exhibits pronounced oscillations of both symmetries (A_{1g} and E_g) in transient optical reflectivity following ultrashort pulse laser excitation [4]. The amplitude of the oscillations, and presumably the atomic displacements, increases with higher excitation strength. Already at intermediate excitation strength, the oscillations in Bi were shown to be nonlinear and time dependent [5]. In this regime, the oscillation frequency is redshifted and, furthermore, chirped [4–11]: As the oscillations damp, their frequencies return to the values obtained in low excitation strength experiments. Explanations of the phenomenon, sometimes referred to as "chirped phonons," mainly pertain to two aspects. One attributes the softening and chirp to lattice anharmonicity induced by high fluence excitation [5,10], stating that when the oscillation amplitude damps with time, the contribution to the frequency originating from the cubic and higher order terms of the lattice potential becomes less pronounced, and hence the potential restores to the range where harmonic approximation applies and the frequency returns to the equilibrium frequency. The other explanation [8,9] ascribes the softening and chirp to a diffusive *e-h* plasma. The screening effect on the bonds between atoms by the photoexcited plasma gradually dies out as the carriers on the excited stratum diffuse into the bulk. In bismuth A_{1g} and E_g phonons both demonstrate chirped frequencies, nonlinear amplitudes, and a fluence-dependent decay rate [4,5,11]. Moreover, for Bi there have been theoretical works which used first-principles density functional calculations to study the effect of lattice anharmonicity and phonon softening by the electron-hole plasma on the fully symmetric phonon dynamics [8,9]. The studies suggested the relative importance of the electronic softening over lattice anharmonicity that was experimentally confirmed by coherent control of the A_{1g} mode [9].

It should be noted that phenomena under high laser fluence excitation have become a popular topic in recent years due to the capability of intense laser radiation to produce a high density plasma and large-amplitude lattice distortions, both capable of triggering photoinduced transient phase transitions [12,13]. Increasing the excitation strength in Bi towards the Lindemann stability limit, it was found that the amplitude of coherent phonon oscillations is fading away, however, at a later time the oscillations can reappear. This phenomenon was initially explained as a quantum mechanical effect and therefore referred to as "amplitude collapse and revival" [14]. The observation of this phenomenon started a discussion as to whether the coherent phonons behave classically as usually assumed, or some quantum effects might contribute to detected signals [14–16]. However, the results of the quantum dynamical simulation carried out as a function of system size suggested that the observed collapse and revival in photoexcited bismuth [15] cannot be ascribed to a quantum mechanical effect, but is most likely of a classical origin. As an alternative explanation, a classical interference between signals reflected from different parts of the crystal (polarization beating) was suggested. Such a mechanism of beats requires the crystal to be excited inhomogeneously, thereby providing the regions with different atomic amplitudes and/or electronic densities. In this paper we have studied the effect of inhomogeneous excitation for large-amplitude A_{1g} phonons in Bi at helium temperature and concluded that lateral inhomogeneity combined with phonon chirp can explain the collapse-and-revival phenomenon, ascribing it to "polarization beating" instead of "quantum beating."

II. EXPERIMENT

The pump-probe experiments were performed in a degenerate pump-probe setup utilizing a 250 kHz regenerative Ti:sapphire amplifier, delivering 50 fs pulses at $\lambda = 800$ nm

(1.55 eV). In a number of the experiments we also used a Ti:sapphire oscillator with 35 fs pulses of the same wavelength and a 80 MHz repetition rate. The induced changes in reflectivity (ΔR) were recorded by a fast-scan technique, enabling a high signal-to-noise level. Crystals were mounted in an optical helium flow cryostat with a silver paste, with both the pump and probe beam entering the sample at near normal incidence. The pump laser beam was polarized along either the trigonal axis in order to avoid the excitation of doubly degenerate phonons, or the bisectrix $[10\bar{1}0]$ axis, and the probe beam was always polarized parallel to the binary $[1\bar{2}10]$ axis. The pump beam diameter was fixed at 100 μm, while the probe diameter was varied between 50 and 100 μm, depending on the experiment type. The background in the fully symmetric signal was removed by a high pass filter with a cutoff frequency of 1.5 THz.

III. EXPERIMENTAL RESULTS AND DISCUSSION

The results of the pump-probe measurements carried out with the same size ($\cong$100 μm) of pump and probe beams are shown in Fig. 1 for four different fluences. The change in reflection is normalized to the reflection in the absence of the pump and shown as a function of the time delay between the pump and probe. At liquid helium temperature and for a pump fluence below 0.15 mJ/cm^2, the amplitude of A_{1g} oscillations is small and increases linearly with excitation strength [4,11]. In this excitation range, the frequency and lifetime of oscillations are independent of the pump fluence and coincide with the frequency-domain data obtained by spontaneous Raman scattering [11,17]. In the time domain, a damped harmonic oscillator model fits well the data for delays up to 100 ps [11]. For the pulses of the regenerative amplifier, the increase in amplitude rapidly becomes nonlinear and the frequency and lifetime of the oscillations begin to depend on time [4–6,11]. Here, the damped harmonic oscillator model fits the data only for the first few cycles while it gradually goes out of phase with later oscillations [11], i.e., the frequency starting at lower frequencies evolves toward higher frequencies as the oscillations damp. The phonon chirp reflects itself in the frequency domain as a line-shape asymmetry, as shown in Fig. 1(b). The fits in real time present such a signal with a low frequency and a short lifetime component for the early time delays and with a longer-lived higher frequency component for the signal at later times [11]. Alternatively, one can fit the signal to

$$A(t) = Ae^{-\Gamma t}\exp[i(\nu t + \varphi(t))], \tag{1}$$

where $\varphi(t) = \beta t^2$ and the instantaneous frequency $\nu_{\text{inst}} = \nu + 2\beta t$ linearly increases in time. The fluence dependence of the phonon frequency and chirp is shown in Fig. 2. In these data, the frequency was determined as the inverse of the average of the first five phonon periods (note that the initial phonon frequency can be considerably lower than the average, and the larger softening corresponds to a larger phonon chirp). For high

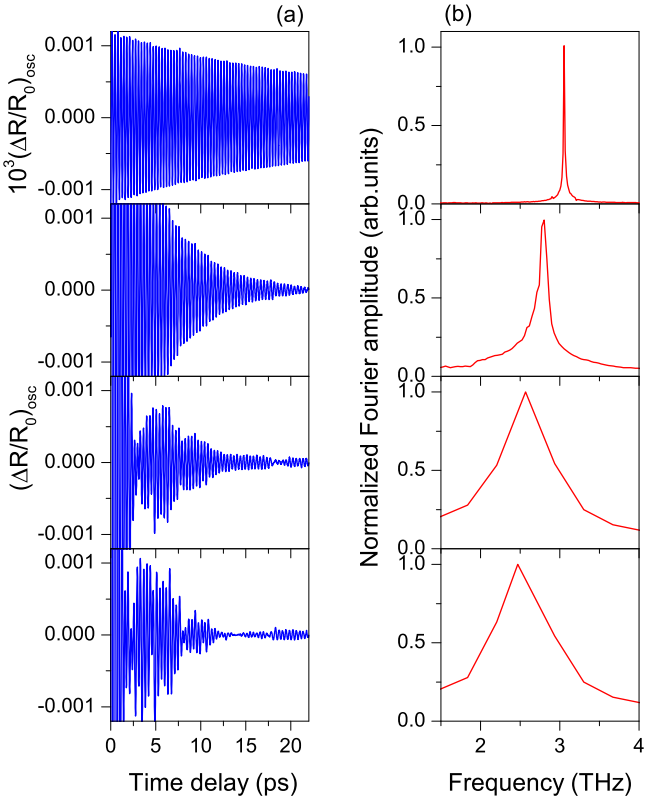

FIG. 1. (Color online) (a) Differential change in reflection in Bi at $T = 5$ K showing the coherent oscillations for different fluences (from the top to the bottom: 0.15, 1.2, 7.9, and 9.4 mJ/cm^2) in the case of equal beam size ($\cong$100 μm) of the pump and probe. Note the different scales for the upper and three lower panels. (b) Normalized fast Fourier transform of the oscillatory signals shown in (a).

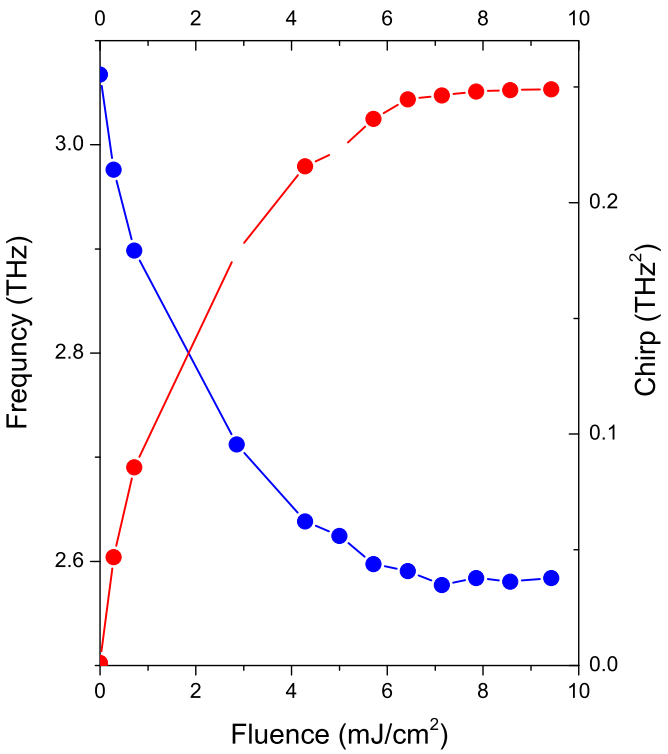

FIG. 2. (Color online) The A_{1g} phonon frequency, obtained from the average period over the first five cycles (left scale), and chirp constant β (right scale) vs pump fluence.

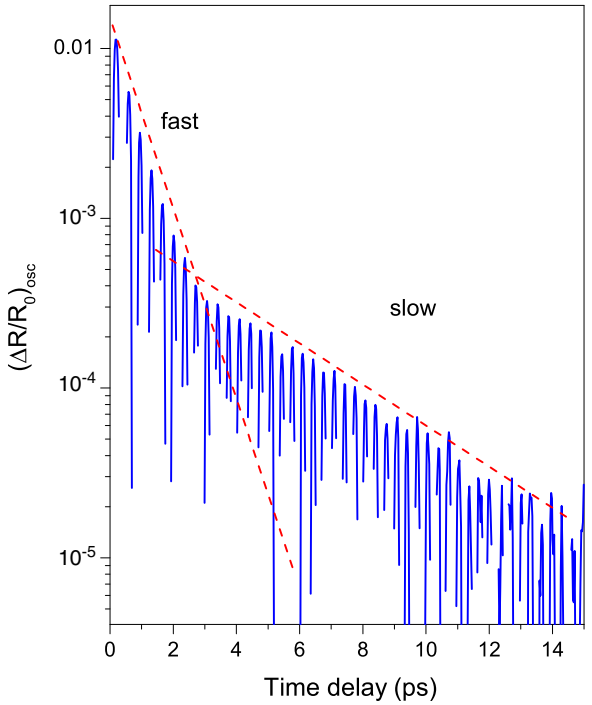

FIG. 3. (Color online) Semilogarithmic plot of the A_{1g} oscillations vs delay time, illustrating biexponential decay. The dashed (red) lines specify the lifetimes of two components.

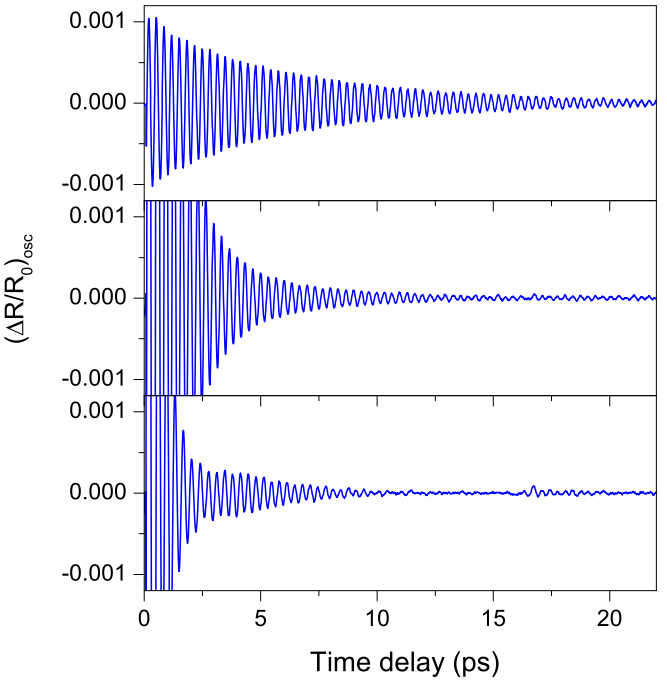

FIG. 4. (Color online) The same as the three lower panels in Fig. 1(a), but in the case when the diameter of the probe beam at the sample position is twice smaller than the diameter of the pump beam to ensure a homogeneous excitation profile.

excitation strengths, the single exponentially decreasing lattice response stepwise changes to biexponential decay [11], which is more clearly seen in the data plotted in a semilogarithmic scale (see Fig. 3). A "new" component, which decays very fast, increases quite rapidly and becomes dominant in the coherent response, because the "old" component saturates for higher fluence. Above a certain threshold the oscillation pattern in Bi changes spectacularly: The oscillations die out, however, at some later time they revive, as shown in Fig. 1(a), exhibiting a collapse-and-revival phenomenon. This behavior was initially explained in terms of the dynamics of a phonon wave packet in an anharmonic potential, where the phonon superposition periodically breaks out and revives to its original form, implying nonclassical dynamics caused by a discrete spectrum [14]. The revival is not perfect, signaling that all the states of the superposition are nearly, but not exactly, in phase. For a higher fluence, as shown in the bottom panel of Fig. 1(a), the oscillations die out only to revive again, demonstrating multiple collapses and revivals with each subsequent revival happening at a progressively larger delay [18].

In attempting to explain the complicated time-resolved lattice response in bismuth, we have to bear in mind that both optically induced lattice distortion and *e-h* plasma density can be strongly inhomogeneous in real space due to nonuniform excitation conditions. To experimentally minimize the lateral inhomogeneity arising due to the excitation with a Gaussian laser beam profile, it is enough to use a probe spot smaller than the pump spot size, thereby sampling only a uniformly excited area. Figure 4 depicts large-amplitude coherent phonon oscillations detected in Bi for approximately the same excitation conditions as in Fig. 1(a). However, the data in Fig. 5 were recorded using a twice smaller probe than the pump spot diameter [which was the same as for Fig. 1(a)] in order to provide more uniform excitation conditions and to investigate spatial variations of the coherent lattice dynamics. By comparing the data, we can easily see that the collapse-and-revival pattern disappears for more uniform excitations. Furthermore, we can scan the pumped area displacing the probe spot along the bisectrix axis, thus detecting differently excited areas (high in the center, low at the edges). Even though in this case each trace exhibits no collapse and revival, the average of these three traces does demonstrate a clear beating

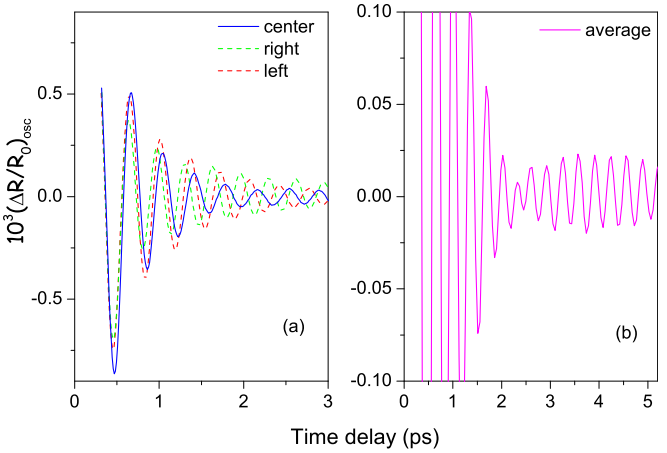

FIG. 5. (Color online) The oscillations detected for three different positions of the probe beam on the pumped area (a) and their average (b).

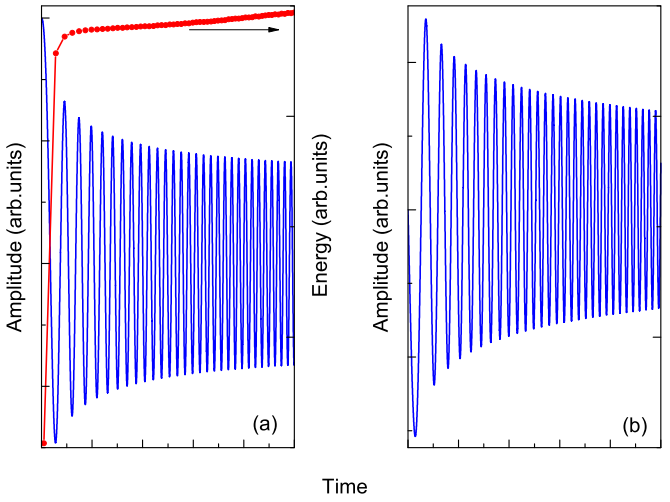

FIG. 6. (Color online) Numerical solutions of Eq. (2) for an oscillator without viscous damping, excited (a) displacively and (b) impulsively. In the left panel the time evolution of the "potential energy" is shown on the right scale.

pattern arising due to different phases of the oscillations, as shown in Fig. 6. This phase difference stems from various phonon chirps that are larger for the central part and smaller at the peripheries of the pumped area. The collapse is reached at a time when the phase variation across the width of the excited area corresponds to $\approx\pi$. This time is somehow inversely proportional to the chirp difference between the center and the edge of the pumped area and therefore will increase for every sequential revival, as it has been observed in experiment [18]. These spatially resolved results demonstrate that the beating observed at high fluence excitation stems from different contributions within the laterally inhomogeneous pumped area. As the initial amplitude, decay rate, and chirp increase while the averaged frequency decreases with fluence, the parameters of the coherent oscillations become dependent on the observation spot. In the center of the pump spot, the chirp is maximal, whereas for the detection spots away from the center, the chirp decreases and, as a result, a plane, uniform phase front of atomic displacements of the excited area evolves with time into a curved one. It should be stressed that the peculiar behavior of the large-amplitude coherent phonons results from phonon chirp. The phonon chirp, that is, a time-dependent frequency, implies that we are dealing with a driven oscillator rather than with a free one. The time evolution of such a driven oscillator crucially depends on an external time-dependent force, which is primarily formed by a diffusive *e-h* plasma. For bismuth, where coherent A_{1g} phonons are generated kinematically (the so called displacive mechanism [19]), this means that apart from the force shifting the potential, one has to take into account the force restoring the potential to the unexcited situation.

Despite the fact that the collapse and revival vanishes for laterally uniform excitations, biexponential decay, phonon softening, and chirp are still present in the data. We now turn to the behavior of the fluence-dependent decay of large-amplitude phonons. In attempting to fully describe the lattice dynamics in a wide range of the used fluences, we are forced to consider two sources of damping for coherent phonons. The first one. Γ_1, which is dominant for low fluence excitation, is analogous to "viscosity friction" on the potential surface, which damps kinetic energy. However, the experimentally observed oscillations can be damped by sources other than the viscous friction. For example, any distribution of frequencies will broaden the spectral line as well as damp the coherent oscillations. Therefore, we have to take into account the damping factor Γ_2 associated with either pure dephasing and/or different potential curvatures that can effectively reduce the oscillations. In order to distinguish this kind of damping from the viscous damping affecting kinetic energy, we will call it potential damping, keeping in mind that in this case the oscillations are damped due to a change in potential energy.

To illustrate the assumptions made let us consider a harmonic oscillator with time-dependent frequency without viscous damping,

$$\ddot{x} + k(1 - e^{-\Gamma_2 t})x = 0, \tag{2}$$

where the overdot represents differentiation with respect to time. The solution in terms of amplitude A and phase θ variables can be written as $x = A(t)\cos[\theta(t)]$, with the amplitude being the solution to the nonlinear differential equation [20]. Taking the oscillator excitation either as kinematic (displacive) or as dynamical (impulsive) and solving Eq. (2) numerically since there is no general analytic solution, we obtain time evolution shown in Figs. 5(a) and 5(b). From this figure, one can see that oscillations damp in time even though the term responsible for viscous damping is missing. One can see that the "potential energy" of the oscillator (taken at the classical turning points) shown in Fig. 5(a) increases in time, reflecting positively chirped frequency. All the peculiarities result from the fact that the amplitude and phase for a time-dependent harmonic oscillator are not uniquely determined variables and the amplitude and frequency may be time dependent and the phase nonlinear with respect to time [20]. Physically this means that the dynamic balance between kinetic and potential energy just after the generation of large-amplitude coherent phonons is to some extent destroyed.

So for the condition $\Gamma_1 \gg \Gamma_2$, which is valid for small initial displacements and low plasma density, the lattice potential in Bi can be well approximated as a harmonic potential with a fixed slope, and the dynamics of the A_{1g} mode resembles a simple, viscosity damped harmonic oscillator. For larger initial displacements and/or plasma density when $\Gamma_1 \ll \Gamma_2$, the oscillatory frequency effectively becomes time dependent, starting at a lower frequency and evolving toward a higher frequency as the oscillations damp.

Now let us try to figure out which factor—anharmonicity or carrier density—controls potential damping, resulting in the biexponential decay. First consider the time-independent anharmonic potential. Since the frequency in the anharmonic potential depends on the initial displacement, any in-depth inhomogeneity, stemming from the fact that the coherent amplitude at the surface is much larger than that at the penetration depth end, can induce a distribution of frequencies through a distribution of initial displacements. Such a distribution of initial displacements has been observed in Bi by employing grazing-incidence femtosecond x-ray diffraction [21]. In the anharmonic potential case, the switch from "fast" to "slow"

damping [11] must occur approximately for the same coherent amplitudes corresponding to the situation when atoms cease to see the anharmonic part of the potential. However, in the experiments [11] we see quite the opposite behavior: The change in the damping rate occurs for larger excitation strengths at smaller amplitudes.

Since the selection rules are modified for the anharmonic potential one can expect to see higher order harmonics in the transient response. The relative amplitude of these harmonics (as compared to the fundamental) must increase as the initial displacements get larger and the atoms sample more anharmonic regions of the potential. The dephasing and viscous damping affecting the damping of the fundamental and its harmonics in a similar fashion tend to decrease the amplitude of the oscillations so that the atoms return to regions of the potential closer to the equilibrium position associated with higher frequencies. At this, the amplitude and phase spectra of the harmonics are expected to follow those of the fundamental [22], i.e., the amplitudes reach a maximum and their phase flips by π at the resonance frequency. To check the behavior of the harmonics we obtain the transient reflectivity of the basal (0001) plane of Bi at intermediate excitation strength, and in Fig. 7 show the amplitude and phase spectra obtained by Fourier transforming the oscillations. Only the first overtone appears in the time-integrated Fourier transform, even though higher order harmonics are present in the short time dynamics studied by a wavelet transformation [18]. The faster decay of the higher order harmonics as compare to that of the fundamental suggests that their damping cannot be due to dephasing in the static aharmonic potential. We infer that some anharmonicity responsible for the appearance of higher order harmonics is present; however, the anharmonicity does not contribute substantially to the potential damping.

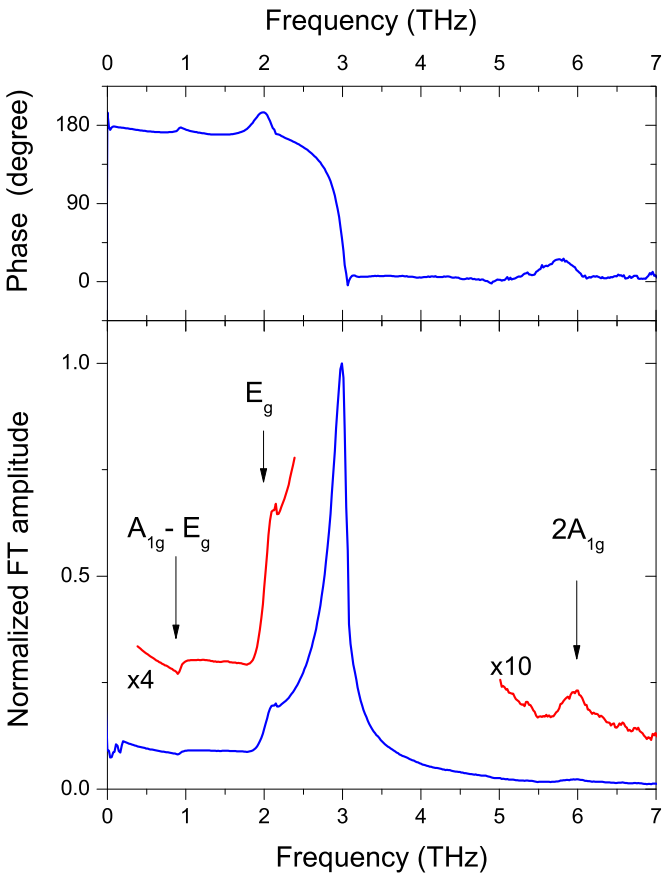

FIG. 7. (Color online) Amplitude and phase spectra of large-amplitude phonons excited on the basal plane [pump and probe polarizations belong to the (0001) plane].

Additionally, a comparison of the phase spectra for the fundamental and its overtone reveal significant differences. Indeed, if the fundamental exhibits expected behavior—its amplitude grows and falls while its phase demonstrates a π flip at the resonance frequency—the phase behavior of the overtone is unusual. Instead of a π flip it exhibits a bump built up around the resonant frequency. Such unusual behavior is unlikely due to second order scattering since a similar trend exists for the phase of the doubly degenerate E_g phonons. The observed features might arise due to phase unwrapping and are not yet fully understood, but, however, seem to be beyond the scope of the present paper.

For the case of the electronic nature of potential damping we must consider two options as the damping term Γ_2 can arise either due to inhomogeneous screening (the carrier density is decreasing along the penetration depth) or to homogeneous, time-dependent screening. In the first case, inhomogeneity of the photoexcited plasma perpendicular to the excited surface has to be considered. Up to now we assumed that one-dimensional (1D) diffusion into the bulk is a dominant effect to control softening and chirp since both effects increase with fluence due to increased injection of the photoexcited carriers, which enhances the screening effect, and we could ignore the lateral carrier diffusion because the typical spot size of 100 μm is much larger than the penetration depth, not exceeding 30 nm for our laser wavelength. The second option for the electronic nature of the potential damping is to take into account the time-dependent, homogeneous potential. The time-dependent potential can be associated with the forces acting on the bismuth atoms following the creation of the *e-h* plasma. It should be stressed that both options will result in time-dependent frequency and additional damping for coherent oscillations.

If the broadening Γ_2 is formed by the inhomogeneous or time-dependent screening resulting from varying slopes of the potentials, the damping associated with such broadening can have stronger effects on the decay of higher harmonics [21], as observed. Therefore, we infer that the main source of the potential damping in Bi is electronic in nature, coming from the photogenerated *e-h* plasma. Additional evidence on the electronic nature of biexponential decay can be found in the comparable phonon chirp lifetime and characteristic decay time of the fast electronic component of the incoherent response [23]. This fact, together with similar resonance profiles for the phonon chirp and the fast electronic component [23], strongly suggest that potential damping Γ_2 is due to varying slopes of potential on which the bismuth atoms move. It should be noted that accurate density functional theory calculations [24] reveal a significant positive contribution to the displacive force due to the cooling of the excited hot electron-hole plasma in TiO_2. In particular, it was shown that this ultrafast evolution of the excited-state potential energy surface could quantitatively explain the experimentally

observed initial phase using reasonable assumptions for the parameters characterizing the excited plasma.

To summarize, a fluence-dependent study of the coherent A_{1g} mode in Bi shows how laser power modifies lattice properties. The high laser power softens the lattice vibrations owing to the screening by a photoexcited plasma. It also causes nonlinear growth of the phonon amplitudes and increased lattice anharmonicity. We demonstrate that near the Lindemann stability limit the collapse-and-revival pattern appears as a result of laterally inhomogeneous excitation. In that case, the beats arise from the interference of polarizations, in which phonon waves do not have a common level, and are different from quantum beats, which have a common level. Our results also demonstrate that a substantial reduction in the lifetime of coherent phonons that is observed when the large-amplitude oscillations are produced cannot be accounted for by a simple harmonic model with viscous damping. Therefore, we suggest a model where the coherent oscillations are damped as the result of inhomogeneity or time dependence of the potential surface. This suggestion needs further testing from a first-principles theoretical consideration and more experimental works to obtain a definite answer on the origin of potential damping.

ACKNOWLEDGMENTS

This work was supported in part by the Russian Foundation for Basic Research through Grant No. 13-02-00263-a. The authors acknowledge K. Ishioka for stimulating discussions and constructive criticism.

[1] For a review, see, e.g., K. Ishioka and O. V. Misochko, in *Progress in Ultrafast Intense Laser Science V*, edited by K. Yamanouchi, A. Giullietti, and K. Ledingham (Springer, Berlin, 2010), pp. 23–64.
[2] R. E. Peierls, in *More Surprises in Theoretical Physics* (Princeton University Press, Princeton, NJ, 1991), p. 24.
[3] A. B. Shick, J. B. Ketterson, D. L. Novikov, and A. J. Freeman, Phys. Rev. B **60**, 15484 (1999).
[4] O. V. Misochko, K. Ishioka, M. Hase, and M. Kitajima, J. Phys.: Condens. Matter **18**, 10571 (2006).
[5] M. Hase, M. Kitajima, S.-I. Nakashima, and K. Mizoguchi, Phys. Rev. Lett. **88**, 067401 (2002).
[6] M. F. DeCamp, D. A. Reis, P. H. Bucksbaum, and R. Merlin, Phys. Rev. B **64**, 092301 (2001).
[7] K. Sokolowski-Tinten, C. Blome, J. Blums *et al.*, Nature (London) **422**, 287 (2003).
[8] S. Fahy and D. A. Reis, Phys. Rev. Lett. **93**, 109701 (2004).
[9] E. D. Murray, D. M. Fritz, J. K. Wahlstrand, S. Fahy, and D. A. Reis, Phys. Rev. B **72**, 060301(R) (2005).
[10] M. Hase, M. Kitajima, S.-I. Nakashima, and K. Mizoguchi, Phys. Rev. Lett. **93**, 109702 (2004).
[11] O. V. Misochko and M. V. Lebedev, J. Exp. Theor. Phys. **109**, 805 (2009).
[12] C. W. Siders and A. Cavalleri, Science **300**, 591 (2003).
[13] D. Fausti, O. V. Misochko, and P. H. M. van Loosdrecht, Phys. Rev. B **80**, 161207(R) (2009).
[14] O. V. Misochko, M. Hase, K. Ishioka, and M. Kitajima, Phys. Rev. Lett. **92**, 197401 (2004).
[15] M. S. Diakhate, E. S. Zijlstra, and M. E. Garcia, Appl. Phys. A **96**, 5 (2009).
[16] O. V. Misochko, Phys. Usp. **56**, 868 (2013).
[17] M. Hase, K. Mizoguchi, H. Harima, S. Nakashima, M. Tani, K. Sakai, and M. Hangyo, Appl. Phys. Lett. **69**, 2474 (1996).
[18] O. V. Misochko, J. Exp. Theor. Phys. **118**, 227 (2014).
[19] H. J. Zeiger, J. Vidal, T. K. Cheng, E. P. Ippen, G. Dresselhaus, and M. S. Dresselhaus, Phys. Rev. B **45**, 768 (1992).
[20] M. Fernández-Guasti, Europhys. Lett. **74**, 1013 (2006).
[21] F. Rosca, A. T. N. Kumar, D. Ionascu, X. Ye, A. A. Demidov, T. Sjodin, D. Wharton, D. Barrick, S. G. Sligar, T. Yonetani, and P. M. Champion, J. Phys. Chem. A **106**, 3540 (2002).
[22] S. L. Johnson, P. Beaud, C. J. Milne, F. S. Krasniqi, E. S. Zijlstra, M. E. Garcia, M. Kaiser, D. Grolimund, R. Abela, and G. Ingold, Phys. Rev. Lett. **100**, 155501 (2008).
[23] A. A. Melnikov, O. V. Misochko, and S. V. Chekalin, J. Appl. Phys. **114**, 033502 (2013).
[24] E. M. Bothschafter, A. Paarmann, E. S. Zijlstra, N. Karpowicz, M. E. Garcia, R. Kienberger, and R. Ernstorfer, Phys. Rev. Lett. **110**, 067402 (2013).